Sādhanā (2018) 43:82
https://doi.org/10.1007/s12046-018-0860-8

Design and analysis of acoustically-driven 50 W thermoacoustic refrigerators

B G PRASHANTHA[1,*], M S GOVINDE GOWDA[2], S SEETHARAMU[3] and G S V L NARASIMHAM[4]

[1]Department of Industrial Engineering and Management, JSS Academy of Technical Education, Dr. Vishnuvardhana Road, Bangalore 560 060, India
[2]Vivekananda College of Engineering and Technology, Nehru Nagar, Puttur, Dakshina Kannada 574 203, India
[3]Formerly Central Power Research Institute, Bangalore 560 080, India
[4]Department of Mechanical Engineering, Indian Institute of Science, Bangalore 560 012, India
e-mail: bgpsandur@gmail.com

MS received 22 September 2017; revised 24 January 2018; accepted 31 January 2018; published online 18 May 2018

Abstract. The design of loudspeaker-driven 50 W cooling power thermoacoustic refrigerators operating with helium at 3% drive-ratio and 10 bar pressure for a temperature difference of 75 K using the linear thermoacoustic theory is discussed. The dimensional normalization technique to minimize the number of parameters involved in the design process is discussed. The variation in the performance of the spiral stack-heat exchangers' at 75% porosity as a function of the normalized stack length and center position is discussed. The resonator optimization is discussed, and the optimized one-third-wavelength (tapered, small diameter tube and divergent section with hemispherical end), and one-fourth-wavelength (tapered and divergent section with hemispherical end) resonator designs show 41.3% and 30.8% improvements in the power density compared to the published 10 W designs, respectively. The back volume gas spring system for improving the performance of the loudspeaker is discussed. The one-third-wavelength and one-fourth-wavelength resonator designs are validated using the DeltaEC software, which predicts the cold heat exchanger temperature of − 3.4 °C at 0.882 COP, and − 4.3 °C at 0.841 COP, respectively.

Keywords. Thermoacoustic; drive ratio; TSDH; TDH; driver; DeltaEC.

1. Introduction

The thermoacoustic refrigeration is the eco-friendly, simple and upcoming technology uses no moving parts and harmful refrigerants compared to the present domestic Vapour Compression Refrigeration (VCR) units. The thermoacoustic refrigerators can be made with the indigenous materials and hence costs less. Thermoacoustic refrigerator works on the concepts of thermoacoustic effect which converts sound energy into refrigeration effect. Thermoacoustic refrigerator systems use loudspeakers to drive themselves and hence these systems are known as Acoustically-Driven Thermo-Acoustic Refrigerators (ADTAR). The ADTAR can make use of the proportional control systems to save the electrical energy input depending on the cooling load. Proportional control system improves overall efficiency by rapid cooling at lower COP and avoiding heat leak losses at higher COP. Whereas the present VCR units use binary control system, it comes on for a while to achieve the desired low temperature and then switched off. The ADTAR systems develop temperature difference across the porous material known as the stack. The stack is made up of the spirally wound thin and low thermal conductivity sheets over the PVC rod with the nylon spacer (fishing line) to facilitate spiral pores along the length of the stack [1, 2]. The porous stack can also be made with other geometries like parallel plates, circular, pin array, etc. [3, 4]. The stack pumps heat from its low temperature end to the other hot end through the oscillating high thermal conductivity gas in the porous stack. The gas oscillates front and back by the acoustic sound wave generated by the loudspeaker. The high frequency oscillation of the gas causes maximum compression and expansion at the hot and cold end of the stack, respectively. The oscillating gas forms the thin thermal conductivity layer along the length of stack to facilitate heat pumping and causes temperature difference across the stack. Hence the thermoacoustic refrigerator makes use of the hot and cold heat exchangers placed on the hot and cold end of the stack, respectively. The Cold Heat Exchanger (CHX) absorbs the

*For correspondence

heat from the cold chamber through the secondary fluid circulating in it and rejects to the surrounding cold gas for heat pumping. The Hot Heat Exchanger (HHX) absorbs the heat from the surrounding hot gas and rejects to the cooling water circulating in it. Therefore to facilitate heat pumping along the stack, it is necessary to install the stack-heat exchangers' assembly in the low thermal conductivity solid resonator tube filled with the working gas. On the left end of the resonator tube the loudspeaker is attached to generate sound waves, and the other end is closed to form the standing wave. The resonator tube can have the geometries like TSDH, TDH, CDH and TSD designs as found in the literature [2, 5]. Among these resonator designs, TSDH and TDH designs are found efficient [2]. An illustration showing the laboratory scale TSDH and TDH resonators designs with the stack-heat exchangers and loudspeaker system are depicted in figure 1.

The loudspeaker is enclosed in the adjustable back volume gas spring systems depending on the operating frequency of the loudspeaker f_d. The loudspeaker with back volume system is known as driver. The back volume system matches the driver frequency f_d with the resonator frequency f to maximize the low electroacoustic efficiency of the commercially available loudspeakers of about 3% to 44.6% [4, 6]. In this paper an attempt is made to design 50 W refrigerators for a temperature difference of 75 K at 3% drive-ratio D (ratio of the dynamic pressure amplitude P_a to its average gas pressure P) and to optimize its components for efficient performance. The objectives of this paper are to theoretically evaluate 50 W refrigerators using linear thermoacoustic theory and to validate its results with the DeltaEC simulation results. The other objectives are to study the performance behaviour of the refrigerator system at 6% drive-ratio using the DeltaEC software with and without stack, and to compare the performance credentials of the present 50 W optimized designs with the 10 W designs found in the published literature [2, 5].

2. Design procedure and normalization of parameters

In this section, a systematic and comprehensive design and normalization procedure of 50 W cooling power loudspeaker driven standing wave refrigerator systems operating at 3% drive ratio for a temperature difference of 75 K is discussed. Because of large number of the design, operating and working gas parameters involved in the design process, it is wise to choose some parameters to simplify the design process. In the design process, there are many parameters to consider which include the operating and working gas parameters, the stack design parameters, the heat exchangers, resonator dimensions and driver parameters. To begin with, a few design choices must be made to reduce the number of variables. Often first step is selecting a working gas because it is much easier to design other parameters around the thermo-physical properties of the working gas. Helium gas is preferred to choose as the working substance because of its highest thermal conductivity and sound velocity compared to all other inert gases. Pure helium gas is cheap in comparison with the other pure and mixture of noble gases. The cost involved in obtaining, storing and mixing of inert gases is relatively high, and the use of the mixture of inert gases shows decrease in cooling power [4]. Next is the selection of the mean operating pressure, it is fairly independent of other parameters and can be easily adjusted as needed. The cooling power and hence power density in thermoacoustic systems can be improved by increasing the average gas pressure P, and the cooling power is proportional to resonator diameter [5, 7, 8]. Also the power density is proportional to resonance frequency [3, 4, 9] and hence higher average operating pressure and frequency is desirable. But increase in the average gas pressure and frequency reduces the stack sheet spacing and hence it is difficult to fabricate the stack [10, 11]. Making a compromise between these two effects, a reasonable 400 Hz frequency and 10 bar average pressure

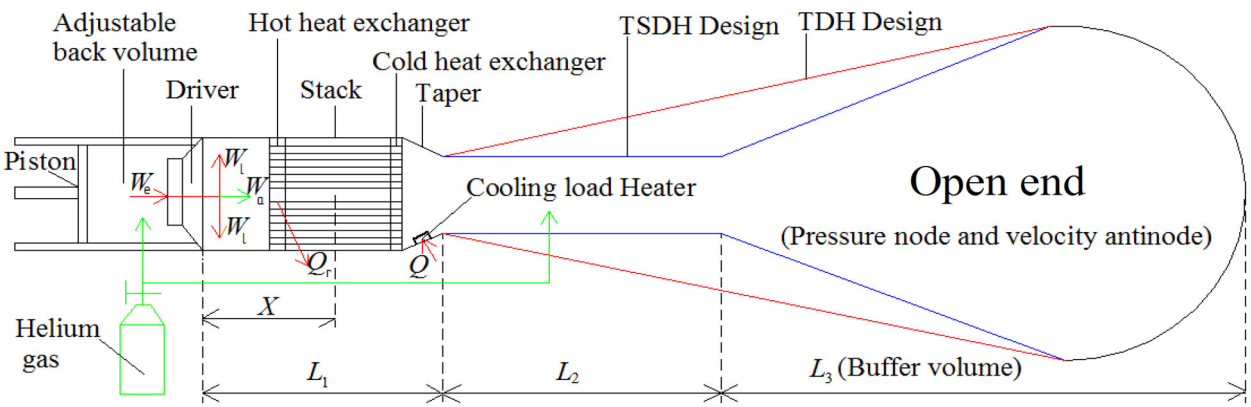

Figure 1. The laboratory scale 50 W cooling power, TSDH and TDH resonators design thermoacoustic refrigerators system.

Table 1. Dependent and independent design parameters of thermoacoustic refrigerator having 50 W cooling power.

Dependent parameters	Independent (normalized) parameters
1. Temperature gradient across stack: θ_x	1. Normalized temperature gradient: $\theta_n = \frac{\theta_x}{T_{mg}}$
2. Mean temperature of gas: T_{mg}	
3. Isobaric specific heat of helium gas: C_{ph}	2. Index of compression: $\gamma = \frac{C_{ph}}{C_{vh}}$
4. Isochoric specific heat of helium gas: C_{vh}	3. Normalized viscous penetration depth: $\delta_{vn} = \frac{\delta_v}{y}$
5. Sound velocity: $u = \sqrt{T_{mg} C_{ph} (\gamma - 1)}$	4. Normalized thermal penetration depth: $\delta_{kn} = \frac{\delta_k}{y}$
6. Resonator operating frequency: f	5. Prandtl number: $\sigma = \left(\frac{\delta_v}{\delta_k}\right)^2 = \frac{\mu C_{ph}}{k_h}$
7. Angular frequency: $\omega = 2\pi f$ rads^{-1}	6. Porosity or Blockage ratio: $\varepsilon = \frac{y}{(y+l)}$
8. Wave number: k	7. Drive-ratio: $D = \frac{P_a}{P}$
9. Average gas pressure: P	8. Normalized stack length: $l_{4n} = kl_4$
10. Viscosity of helium: μ	9. Normalized stack centre position: $X_n = kX$
11. Density of helium: ρ	10. Normalized cooling power of the stack: $Q_{ns} = \frac{Q}{(PuA)}$
12. Viscous penetration depth of helium: $\delta_v = \sqrt{\frac{2\mu}{\rho\omega}} = \sqrt{\frac{2\mu}{\rho(2\pi f)}}$	11. Normalized acoustic power of the stack: $W_{ns} = \frac{W_s}{(PuA)}$
13. Thermal conductivity of helium: k_h	
14. Thermal penetration depth of helium: $\delta_k = \sqrt{\frac{2k_h}{\rho C_{ph}(2\pi f)}}$	
15. Half stack sheet spacing: $y = 2\delta_k$	
16. Half stack sheet thickness: l	
17. Dynamic pressure amplitude: P_a	
18. Stack length: l_4	
19. Stack center position: X	
20. Cooling power: Q	
21. Cross-sectional area of stack: A	
22. Acoustic power consumed by the stack: W_s	

is chosen. For the purpose of avoiding severe nonlinearities in the system and to obtain better modelling accuracy for the standing wave refrigerators, it is suggested that the drive-ratio, D must be $\leq 3\%$. Such systems are generally termed as low amplitude thermoacoustic systems [12]. Even after these preliminary choices, the stack is an appropriate place to begin, as it is often difficult to machine and construct a stack to meet predetermined specifications. Once the stack material and geometry is chosen, the CHX, HHX and the resonator system can be designed accordingly. Finally, an appropriate loudspeaker can be chosen.

The popular dimensional normalization technique is used to reduce the total number of parameters involved in design process [13]. The design of a refrigerator system depends on large number of dependent parameters, which can be grouped under stack geometrical parameters, material specific parameters and design requirement parameters [2, 14]. The stack geometrical parameters are: stack position and length, plate spacing and thickness, and cross sectional area. The working gas and stack material specific parameters include: thermo-physical properties of the working gas and the stack density, specific heat and thermal conductivity. The design requirement parameters are given by: resonance frequency, average gas pressure, dynamic pressure amplitude of the working gas, mean temperature, the required temperature gradient across the stack heat exchangers system and the required cooling power. It is laborious to deal with the twenty two dependent parameters as listed in table 1. Using parameters normalization technique, the total number of parameters involved in the design process is reduced to eleven independent parameters (table 1). The normalized thermal and viscous penetration depths for most of the linear thermoacoustic models are found to be in the range of 0.5–1 and $0.5\sigma^2$ to σ^2, respectively [15]. The porosity (also called as blockage ratio) ε of the stack-heat exchangers system recommended in the literature for the linear thermoacoustic model was set equal to 0.75 [4].

3. Design and optimization of spiral stack-heat exchangers system, and resonator system

In this section, the design and optimization of spiral stack-heat exchangers system, and resonator systems of 50 W refrigerators at 3% drive-ratio for a temperature difference

of 75 K are discussed. The most important term which decides performance of the refrigerator system is the critical temperature difference across the stack is also discussed. The results of spiral stack performance as a function of the normalized stack center position, and stack length, and the variation of design and performance parameters as a function of the normalized stack center position, and length are also notified and detailed. And the design and analysis of the TSDH and TDH resonator designs are discussed.

3.1 *Design and optimization of a 50 W spiral stack-heat exchangers system*

The stack is considered as the heart in the stack-based thermoacoustic refrigerators because the performance of the whole refrigerator greatly depends on the stack itself. The stack pumps heat from its cold end to hot end through the pores of the spirally wound stack sheet material. The rate of stack heat pumping depends on the thermal conductivity and the velocity of the oscillating gas. The stack sheet material conducts the heat in the direction opposite to the stack heat pumping (from hot end of the stack to cold end), which decreases the performance of the stack [3, 4]. Hence it is a wise choice to select the stack sheet material with low thermal conductivity, and the heat capacity much greater than the heat capacity of working gas for its long life. Therefore the locally available Mylar sheet meets the design requirements. The stack can have different geometry viz. spiral pores, parallel plates, circular pores, pin arrays, triangular pores, etc. In this research work, the thin spiral pores stack geometry is chosen since it is easy to manufacture and takes less time compared to other geometries. The thin Mylar sheet thickness (2 l) is first glued over the 6 mm PVC rod and then wrapped over it using Nylon fishing line provided along its length acts as a spacer for the oscillating gas as shown in figure 2. The Mylar sheet thickness and the spacer distance ($2y$) are calculated based on the required porosity of the gas ε.

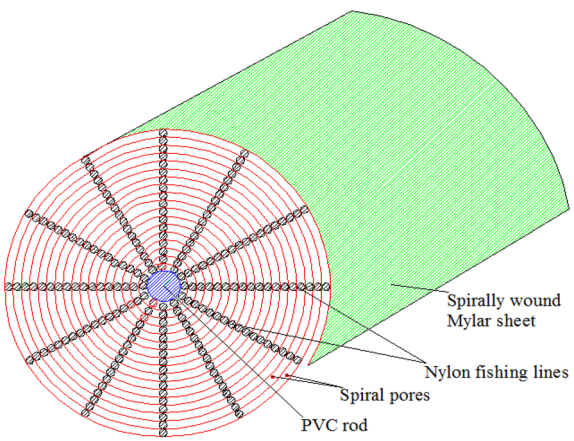

Figure 2. Schematic showing the spirally wound stack with spiral pores.

Critical Temperature Difference: In standing wave thermoacoustic devices, the most important term which decides performance of the stack is the critical temperature θ_c.

At critical temperature either in the case of thermoacoustic refrigerator or engine, heat is not transferred through the stack because of zero temperature difference θ_x across the stack. The critical temperature is defined as the ratio of change in temperature T_1 to the displacement amplitude of the gas parcel x_1 at a particular location. Using the equations of the amplitude of pressure and velocity inside the resonator tube at a distance x measured from the loudspeaker position equations: $p_1 = P_a\cos(kx)$ and $u_1 = (P_a\sin(kx) \div \varepsilon\rho u)$, and substituting $(\omega \div u) = k$, the critical temperature θ_c is given by:

$$\theta_c = \frac{T_1}{x_1} = \left(\frac{\frac{p_1}{\rho C_p}}{\frac{u_1}{\omega}}\right) = \frac{\varepsilon u\omega\cot kX}{C_p} = \frac{\varepsilon u\omega\cot kX}{\left(u^2 \div T_{mg}(\gamma-1)\right)} = (\gamma-1)\varepsilon kT_{mg}\cot kX \quad (1)$$

The critical temperature difference across the stack is measured per unit length of the stack. Another important term called normalized temperature difference Γ which decides the thermoacoustic device is a refrigerator, engine or a neutral system. The normalized temperature difference is defined as the ratio of the temperature difference across the heat exchangers θ_x to its critical temperature difference θ_c. The normalized temperature difference Γ per unit length of the stack using parameters normalization technique (table 1): $\theta_x \div T_{mg} = \theta_n$, $kl_4 = l_{4n}$, and $kX = X_n$, is given by

$$\Gamma = \frac{\theta_x}{\theta_c} = \frac{\theta_n \tan X_n}{(\gamma-1)\varepsilon l_{4n}} \quad (2)$$

For any standing wave thermoacoustic system, if θ_x is greater than θ_c then Γ is greater than one then heat flows from the hot end of the stack to the cold end, generating acoustic sound wave (engine). And if θ_x is less than θ_c, then Γ is less than one then stack pumps heat from the cold end of the stack to the hot end (refrigerator) upon acoustic power input. And if Γ is equal to one, then no heat flows across the stack.

In the literature [9, 16] the mathematical steps involved in designing a theoretical model for the loudspeaker driven thermoacoustic refrigerators are presented. Both the authors have given different normalized heat and work flux equations. In this research work, we have derived the normalized heat flux and work flux equations for the spiral pores stack considering the stack thermal conductivity factor from Rott's governing thermoacoustic equations [3]. The Rott's governing thermoacoustic heat flux equation and acoustic power equations are given by:

$$Q = \frac{-\Pi\delta_k}{4}\frac{T_m\beta p_1 u_1}{(1+\epsilon_s)(1+\sigma)\Lambda}\left[\Gamma\frac{1+\sqrt{\sigma}+\sigma+\sigma\epsilon_s}{1+\sqrt{\sigma}} - \left(1+\sqrt{\sigma}-\frac{\delta_v}{y}\right)\right] - \Pi(yK+lK_s)\frac{T_m}{l_4} \quad (3)$$

The terms in the right hand side of the above equation represents the thermoacoustic heat conduction through the working gas and stack material.

$$W = \frac{\Pi l_3}{4}\left[\frac{\delta_k(\Upsilon-1)\omega p_1^2}{\rho u^2(1+\epsilon_s)}\left(\frac{\Gamma}{(1+\sqrt{\sigma})\Lambda}-1\right) - \frac{\delta_v\omega\rho u_1^2}{\Lambda}\right] \quad (4)$$

Here Λ is the heat energy conduction correction factor for the given operating gas which is defined as

$$\Lambda = 1 - \frac{\delta_v}{y} + 0.5\frac{\delta_v^2}{y^2} \quad (5)$$

The first and second terms in Eq. (4) are referred to as the thermal and viscous relaxation dissipation terms for the operating gas, respectively. For an ideal stack, the stack thermal conductivity K_s and heat capacity ratio ϵ_s (which is the ratio of the heat capacity of the working gas to the heat capacity of the stack material) are assumed to be zero. Assuming the working gas (helium) behaves like an ideal gas such that the product $T_m\beta$ is equal to one. Substituting the equations for u, ε, σ, δ_v and δ_k given in table 1, and $\Pi = A/(y + l)$, $p_1 = P_a\cos(kx)$ and $u_1 = P_a\sin(kx)/\varepsilon\rho u$ and using the definitions of the normalized parameters into Eqs. (3) and (4). Dividing Eqs. (3) and (4) by the product (PuA), and taking the hydraulic radius equal to half-stack spacing ($r_h = y$), then the normalized heat power output equation $Q_{n\text{-}s}$ and work power input equation $W_{n\text{-}s}$ with circular pores stack are given by:

$$Q_{n-s} = \frac{-\delta_{kn}D^2\sin(2X_{n-s})}{8\gamma(1+\sigma)\Lambda} \times \left[\Gamma\frac{1+\sqrt{\sigma}+\sigma}{1+\sqrt{\sigma}} - \left(1+\sqrt{\sigma}-\sqrt{\sigma}\delta_{kn}\right)\right] - \varepsilon\Lambda^1. \quad (6)$$

The term Λ^1 in Eq. (6) is the normalized helium gas thermal conductivity factor which is given by:

$$\Lambda^1 = \frac{K_h T_{mg}}{Pul_3} \quad (7)$$

and

$$W_{n-s} = \frac{\delta_{kn}l_{3n}D^2}{4\gamma}\left[(\gamma-1)\varepsilon cos^2(X_{n-s})\left(\frac{\Gamma}{(1+\sqrt{\sigma})\Lambda}-1\right) - \frac{\sqrt{\sigma}sin^2(X_{n-s})}{\varepsilon\Lambda}\right] \quad (8)$$

Using the normalized Eqs. (6)–(8), the stack COP for the refrigerator system is given by:

Table 2. Dependent and independent parameters data used in the design process.

Dependent parameters	Independent parameters
θ = 75 K, T_{mg} = 266 K, C_{ph} = 5.2 kJ kg^{-1} K^{-1}, C_{vh} = 3.1 kJ kg^{-1} K^{-1}, u = 960 ms^{-1}, f = 400 Hz, k = 2.62 rad m^{-1}, P = 10 bar, μ @ T_{mg} = 1.8372 × 10^{-5} kg m^{-1} s^{-1}, ρ @ T_{mg} = 1.8097 kg m^{-3}, δ_v = 0.089882 mm, k_h @ T_{mg} = 0.13985 W m^{-1} K^{-1}, δ_k = 0.10882 mm, y @ $2\delta_k$ = 0.2176 mm, l = 0.0725 mm, P_a = 0.3 bar, l_4 = 76 mm, X = 76 mm, Q = 10 W, A = 0.007498 m^2, W_s = 31.3 W	θ_n = 0.282, γ = 1.67, δ_{vn} = 0.4131, δ_{kn} = 0.5, σ = 0.68, ε = 0.75, D = 0.03, l_{4n} = 0.2, X_n = 0.2, Q_{ns} = 6.946 × 10^{-6}, W_{ns} = 4.348 × 10^{-6}

$$COP_s = \frac{Q_{n-s}}{W_{n-s}} \quad (9)$$

Let d_1 be the diameter of the large resonator tube neglecting stack holder thickness which is much smaller than d_1. The large resonator tube holds the stack-heat exchangers system. The "large resonator tube diameter" also known as "stack diameter" d_1 is found from the stack cross-section A. The stack cross-section A is found from the design optimization of the spiral stack.

Determination of the stack cross-section A: Using data given in table 2 in Eqs. (6)–(8), the stack COP is determined using Eq. (9). The spiral stack performance COP_s versus various normalized stack length l_{4n} and center position $X_{n\text{-}s}$ are given in table 3.

The selection of the optimal stack length l_4 and centre position X helps the designer in providing sufficient space to accommodate the loudspeaker, pressure and temperature sensors during fabrication. The selection of the optimum stack length and center position is decided based on the performance of the stack (COP_s) itself. Highest performance of the stack consumes lowest acoustic power input and vice-versa. Improvement in the stack performance improves cooling power and hence the performance of the whole refrigerator system. Based on the above discussion it is decided to select the best normalized stack length (l_{4n}) and centre position (X_n) as 0.2. The optimized stack COP at this condition is found to be 1.598. Substituting the value of k (wave number) from table 2 in the normalized stack length and center position equations (table 1), the stack length and centre position is found to be 76 mm. It is as good as keeping the hot end of the stack at a distance 38 mm away from the loudspeaker position. Substituting the known data in Eq. (6), the normalized cooling power $Q_{n\text{-}s}$ is given by 6.946 × 10^{-6}. The stack cross-section A is calculated by substituting the given data (table 2) in the

Table 3. Spiral stack performance results as a function of the normalized stack center position and stack length.

	X_{ns}				
COP_s	0.1	0.2	0.3	0.4	0.5
l_{4n}					
0.1	1.576	− 3.773	54.1	39.98	51.6
0.2	1.058	**1.598**	0.892	− 1.425	− 4.718
0.3	0.744	1.256	1.303	0.831	− 0.003
0.4	0.571	0.996	1.144	0.998	0.629
0.5	0.463	0.818	0.982	0.939	0.738

Bold value represent the "optimized design value".

equation $Q_{n\text{-}s} = Q \div (PuA)$. And using the stack cross-section A, the stack diameter d_1 is found to be 98 mm. Similarly, the normalized acoustic power ($W_{n\text{-}s}$) 4.348×10^{-6} is found using Eq. (8). The acoustic power consumed by the stack W_s for pumping 50 W of heat load is calculated using the equation $W_{n\text{-}s} = W_s \div (PuA)$ is found to be 31.3 W (table 4).

Heat Exchangers Design: Heat exchangers namely the CHX and HHX are placed in close contact with the cold end and hot end of the stack, respectively as shown in figure 1. The CHX absorb the heat from the cold chamber (source) to produce refrigeration effect and the same heat is pumped to the HHX through the stack upon the acoustic power W supplied by the loudspeaker into the resonator system. The circulating cooling water removes the heat from the HHX to the atmosphere (sink). The cold and hot heat exchangers are made from very thin copper sheets (0.145 mm) spirally wound over a 6 mm copper rod as shown in figure 3. The thin copper fishing line (0.435 mm) acts as spacer line for the oscillating gas. The porosity ε (0.75) and diameter d_1 (98 mm) for both the CHX and HHX is assumed to be same as that of the spiral stack.

But the lengths of the cold and hot heat exchangers are calculated based on the peak-to-peak displacement amplitude of the gas x_1 at their locations, which can be calculated using:

$$x_1 = \frac{u_1}{\omega} = \frac{P_a \sin(kx)}{\varepsilon \rho u \omega} \tag{10}$$

In the literature [4, 9], the acoustic displacement amplitude equation (Eq. (10)) is used in calculating the length

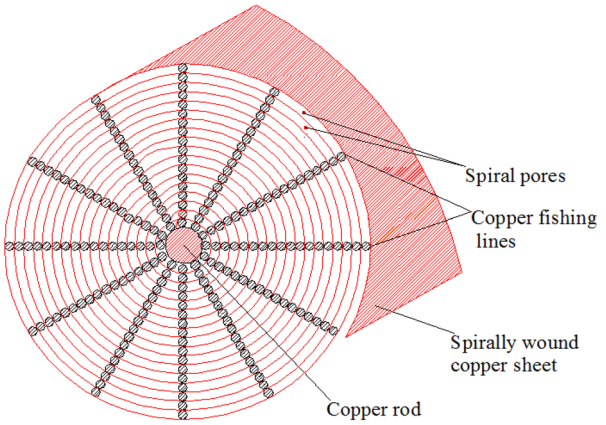

Figure 3. Schematic showing the spirally wound copper heat exchanger with spiral pores.

of the heat exchangers neglecting the porosity ε (0.75). Referring to Eq. (10), the acoustic displacement amplitude of the gas x_1 varies inversely with gas porosity ε. The heat exchangers consume more acoustic power input as the calculated length of the heat exchangers increases at 75% porosity (ε) and slightly affect the acoustic field and hence the refrigerator performance. From the literature [3, 16] it is found that the heat exchangers length is two times the acoustic displacement amplitude of the gas x_1. Substituting the position of the CHX away from the loudspeaker (x = 114 mm) and data given in table 2 in Eq. (10), the linear displacement x_1 is found to be 3 mm. Therefore the length of the CHX $2x_1$ is equal to 6 mm. At this condition, the normalized length (l_{5n}) and position ($X_{n\text{-}cx}$) of the CHX is found to be 0.0157 and 0.3065, respectively. Substituting data given in table 2, and putting the normalized temperature gradient equal to zero ($\Gamma = 0$) in Eq. (8) because of the small length of heat exchangers, the acoustic power W_{cx} dissipated in the CHX is found to be 4.614 W. The HHX has to reject the heat to the atmosphere through the cooling water circulating inside the copper tubes of the HHX. In the literature [3, 4] it is stated that the HHX has to remove nearly equal to two times the heat supplied by the CHX. Hence the length of the HHX is about two times the length of CHX and therefore it is found to be 12 mm. The normalized length (l_{3n}) and position ($X_{n\text{-}hx}$) of the HHX is found to be

Table 4. Variation of design and performance parameters as a function of the normalized stack center position and length.

$X_{ns} = l_{4n}$	d_1 (mm)	l_1 (mm)	l_2 (mm)	l_3 (mm)	l_4 (mm)	l_5 (mm)	W_s (W)	W_{cx} (W)	W_{hx} (W)	W_{sx} (W)
0.1	148	19	13	6	38	3	31.7	4.629	8.833	45.2
0.2	**98**	38	26	12	**76**	6	31.3	4.614	7.784	**43.7**
0.3	81	57.5	42	16	115	8	38.4	5.073	7.254	50.7
0.4	73	76.5	55	22	153	11	50.1	6.783	8.259	65.1
0.5	68	95.5	70	26	191	13	67.7	8.495	8.993	85.2

Bold values represent the "optimized design values".

0.0314 and 0.0838, respectively. Similar to CHX, the acoustic power W_{hx} dissipated in the HHX is calculated using Eq. (8) is found to be 7.784 W. In table 4 it is found that the total acoustic power consumed in the stack-heat exchangers system (W_{sx}) is lowest 43.7 W at $X_{ns} = l_{4n-} = 0.2$, and hence the selection of the stack length and centre positions at 76 mm is justified.

3.2 *Design and analysis of resonator system*

The resonator is designed such that the length, mass, losses and shape are at the optimum level. The resonator tube should be strong enough to sustain pressure greater than or equal to 10 bar and has good surface finish to reduce the heat dissipation losses. The resonator must be made from the low thermal conductivity material to minimize the heat dissipation losses [17, 18]. The performance of the refrigerator system improves with decrease in resonator heat dissipation losses. Also the ambient heat may leak into the CHX section of the resonator tube with the normal insulation. Hence it is advisable to keep the resonator system under vacuum or to provide multi-layered-super-insulation to attenuate heat leak losses. From the literature [3, 4, 17], it is learnt that one-fourth-wavelength resonator tube losses are 50% lower than the half-wavelength resonator tube. The total length of the one-fourth-wavelength resonator tube is found by:

$$L_t = \frac{0.25u}{f} \tag{11}$$

The one-fourth-wavelength resonator tube with the same large diameter tube d_1 throughout its length has resonator losses. Therefore the attempts are made in this paper to reduce the resonator losses by decreasing the cross-section of the resonator tube right side to the CHX. The cross-section right side to the CHX is roughly up to 75% of the resonator length measured from the loudspeaker position or which is approximately the middle portion of the resonator tube, is decreased to reduce the resonator losses. Let d_2 be the diameter of the small (reduced) tube. The small length 20 mm taper is used to connect the large and small diameter tubes. The total acoustic power loss as heat load along the length of the small diameter tube d_2 is given by [17]:

$$W_2 = \frac{d_2}{d_1}\left(\frac{\cos(kx_A)}{\cos\left(kx_A^1\right)}\right)^2\left[\left(1+\frac{\gamma-1}{\sqrt{\sigma}}\right)\left(kx_B^1 - kx_A^1\right) + 0.5\left(1-\frac{\gamma-1}{\sqrt{\sigma}}\right)\left(\sin\left(2kx_A^1\right) - \sin\left(2kx_B^1\right)\right)\right]\frac{\pi d_1 \delta_v u P_a^2}{8\gamma P} \tag{12}$$

where kx_A is the normalized large diameter tube length and kx_A^1 is the normalized large diameter tube length at diameter-ratio d_2/d_1 which is given by:

$$kx_A^1 = \tan^{-1}\left(\left(\frac{d_1}{d_2}\right)^2 \tan(kx_A)\right) \tag{13}$$

In Eq. (12), the two subscripts 'A' and 'B' refers to the two transition points. Subscript 'A' is for between d_1 and d_2 and subscript 'B' is referred to the transition point between d_2 and the buffer volume. The buffer volume is large and it simulates an open end. The acoustic pressure attains maximum and the velocity is zero at the loudspeaker closed end. The total acoustic power loss W_2 as heat load along the length of the small diameter tube d_2 versus diameter ratio d_2/d_1 is calculated using Eq. (12) as given in table 5.

The W_2 losses in the small diameter tube d_2 is minimum at $d_2/d_1 = 0.8$. At this diameter ratio, the thermal and viscous losses in the small diameter tube are minimal. The diameter-ratio $d_2/d_1 = 0.8$ is used in this work while designing a 50 W refrigerator at 3% drive-ratio for the temperature difference of 75 K. Let L_1 be the length of the large tube d_1 and x is the position away from the loudspeaker. At the interface between d_1 and d_2 (at $x = L_1$), the pressure and velocity distributions should be continuous. Let Z_1 and Z_2 are the acoustic impedances in d_1 and d_2, respectively and are made equal at $x = L_1$ as given below.

$$Z_1 = \frac{P_1}{A_1 u_1} = Z_2 = \frac{P_2}{A_2 u_2} \tag{14}$$

Where $P_1 = P_a\cos(kL_1)$, $u_1 = P_a\sin(kL_1)/\rho u$, $P_2 = P_a\sin(kL_2)$ and $u_2 = P_a\cos(kL_2)/\rho u$, L_2 is the length of d_2 and by substitution:

$$\cot(kL_1) = \left(\frac{d_1}{d_2}\right)^2 \tan(kL_2) \tag{15}$$

Using data given in table 2 in Eq. (11), the total length of the one-fourth-wavelength resonator tube (L_t) is found to be 600 mm per cycle. Let L_1 be the length of d_1. Considering the positions of the HHX, stack, CHX and the taper away from the loudspeaker in the resonator tube and summing their lengths, the total length of the large diameter tube L_1 is found to be 140 mm as depicted in figure 4.

Substituting the known data in Eq. (15), L_2 is given by 390 mm and let L_3 is the length of the buffer volume. After knowing L_t, L_1 and L_2, the buffer length L_3 is found to be 70 mm. From the literature [3, 4, 17] it is found that the volume of the buffer (V_b) is approximately about seven times the volume left to taper (VLT), which simulates an open end in the buffer length. Therefore, at this approximation we have set the V_b and volume right to taper (VRT)

Table 5. Variation of the total acoustic power loss in the small diameter tube as a function of the diameter ratio.

d_2/d_1	0.2	0.4	0.6	**0.8**	1
W_2 (W)	10.903	5.734	4.540	**4.526**	4.991

Bold values represent the "optimized design values".

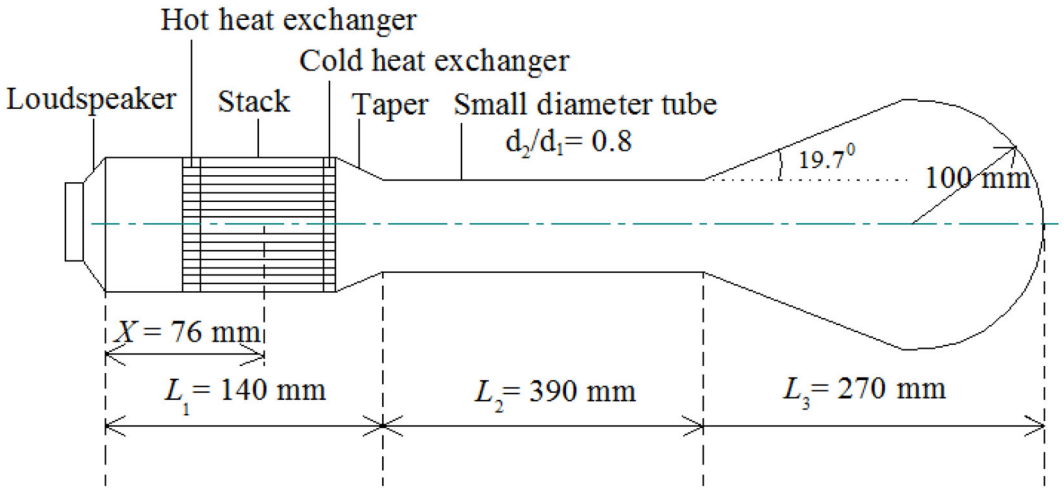

Figure 4. Optimized λ/3-TSDH resonator design for a temperature difference of 75 K having 50 W cooling power.

for the 50 W resonator tube (figure 4) are equal to 4.85 L and 6.73 L, respectively. At this condition, the diverging angle θ_2 in the buffer length and total length L_t for the optimized 50 W 0.33λ-TSDH resonator design is found to be 19.7° and 800 mm, respectively. Dividing Eq. (4) by Πl_3 (stack surface area), setting $\Gamma = 0$, neglecting the stack plate heat capacity-ratio ϵ_s, and considering the half-stack spacing y $\gg \delta_k$, we get an equation for the acoustic power loss per unit surface area of the resonator tube w, which is given by:

$$w = 0.25\rho_h u_1^2 \delta_v \omega + 0.25 \frac{p_1^2(\gamma - 1)\delta_k \omega}{\rho_h u^2} \tag{16}$$

The first and second terms in the right-hand side of Eq. (16) represents the viscous and thermal losses in the resonator system. The pressure p_1 and velocity u_1 in Eq. (16) are calculated at the mean centre positions of the components in the resonator tube measured from the loudspeaker position. For example: the pressure p_1 and velocity u_1 at the mean centre position of the duct between the loudspeaker and HHX, and similarly at the mean centre positions of the HHX, stack, CHX, taper, small diameter tube length, divergent section, and at the hemisphere. The acoustic power lost by each resonator component (w_{rc}) is obtained by multiplying Eq. (16) by an individual component surface area. The total resonator surface area A_t for the λ/3-TSDH resonator design (figure 4) is found to be 2810 cm^2. The total acoustic power lost as heat by the TSDH resonator design W_r is found to be 8.1 W, which is obtained by adding the calculated individual resonator components acoustic power loss (w_{rc}). The total acoustic power utilized by the stack, heat exchangers and the resonator system W_t, and the COP, COPC, and COPR for the 50 W refrigerators are obtained by:

$$W_t = W_s + W_{cx} + W_{hx} + W_r \tag{17}$$

$$\text{COP} = \frac{Q}{W_t} \tag{18}$$

$$\text{COPC} = \frac{T_{cx}}{T_{hx} - T_{cx}} \tag{19}$$

$$\text{COPR} = \frac{\text{COP}}{\text{COPC}} \tag{20}$$

The total volume of the resonator V_t and hence the power density P_v for the λ/3-TSDH resonator design are found to be 7.757 L and 6446 Wm^{-3} respectively as given in table 6. Further, the attempts are made to improve the performance (COP) and power density (P_v) for the λ/3-TSDH resonator design by reducing A_t, VRT, and V_t. Therefore an alternate, efficient and compact λ/4-TDH resonator design is proposed as shown in figure 5. The alternate λ/4-TDH resonator design is found to be efficient compared to the λ/3-TSDH resonator design (table 6). For the λ/4-TDH design, the diameter-ratio d_2/d_1 at the interface between the taper and divergent sections is chosen to be 0.2 and hence the throat diameter d_2 is found to be 19.6 mm. The radius of the hemispherical end is chosen to be 100 mm to minimize the resonator losses.

By restricting the total length of the resonator tube (L_t) to 600 mm to make the device compact, the diverging angle in the buffer length θ_2 is found to be and 14.1°. The calculated total resonator loss (W_r) for the λ/4-TDH resonator design is found to be 6.6 W, which is lower compared to the λ/3-TSDH resonator design (table 6). Therefore, the COP and COPR for the λ/4-TDH resonator design are comparatively higher. The design and performance credentials of the present 50 W TSDH and TDH resonator designs and the published 10 W TSDH and TDH resonator designs [2] are also given in table 6. The 50 W resonator designs are found to be efficient compared to the 10 W resonator designs in terms of power density and COP.

Table 6. Theoretical design and performance credentials of the TSDH and TDH 10 W and 50 W resonator designs.

Resonator Design	L_t (mm)	d_2 (mm)	VLT (L)	VRT (L)	A_t (cm^2)	V_t (cm^3)	P_v (W m^{-3})	θ_2 (°)	W_r (W)	COP	COPR
λ/3-TSDH @ 50 W	800	78.4	0.905	6.73	2810	7757	6446	19.7	8.1	0.966	0.322
0.28λ-TSDH @ 10 W	650	37.2	0.512	1.7	1297	2192	4563	19	3.4	0.435	0.288
λ/4-TDH @ 50 W	600	19.6	0.905	6.27	2359	7238	6909	14.1	6.6	0.994	0.331
0.24λ-TDH @ 10 W	556	12.4	0.512	1.4	1130	1893	5282	8	2.9	0.444	0.294

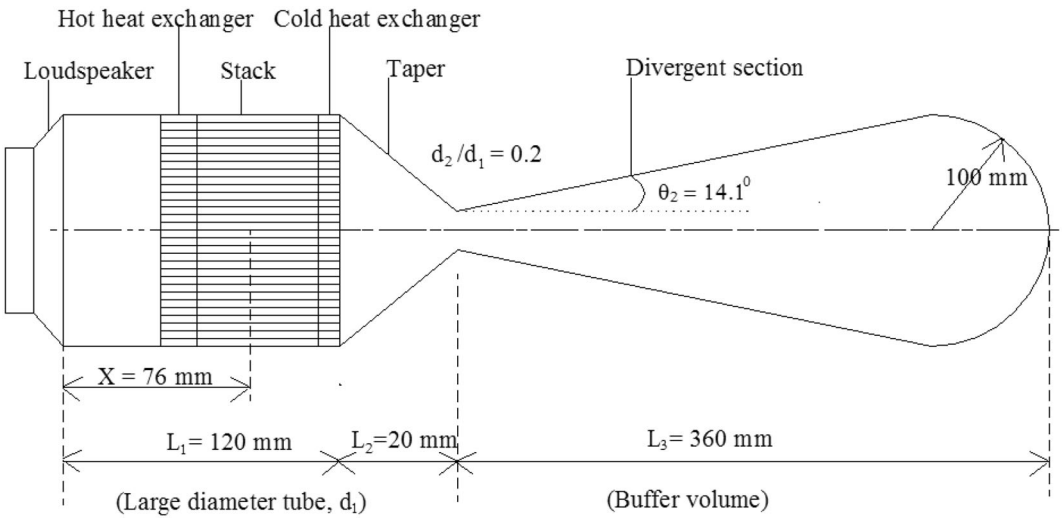

Figure 5. An alternate 50 W cooling power λ/4-TDH resonator designed for a temperature difference of 75 K.

The stack length l_4 (76 mm) is much smaller compared to the wavelength λ (2400 mm per cycle). Hence the first short stack assumption of the linear theory is perfectly satisfied. Therefore placing the stack-heat exchangers system with porosity (ε) 0.75 does not have any significant effect on the acoustic field. It is also found that the half stack spacing $y >> \delta_v, \delta_k$, satisfies the second assumption (boundary layer approximation) of the linear theory. Referring to table 2, the 50 W refrigerator is designed at θ_x = 75 K and T_{mg} = 266 K that is $T_{mg} >> \theta_x$, the temperature difference across the heat exchangers θ_x is almost 28.2% of T_{mg}. Hence the thermophysical properties of helium gas along the length of the stack remains constant. This satisfies the third assumption of the linear theory. Therefore the three important assumptions of a linear thermoacoustic theory are perfectly satisfied [3]. Using Eqs. (1) and (2), the critical temperature gradient (θ_c) and the normalized temperature gradient (Γ) are found to be 131.3 K and 0.5688, respectively, which satisfies the primary requirement of the device to behave as a refrigerator ($\Gamma < 1$) [15].

4. The back volume gas spring system for an acoustic driver

The back volume gas spring system is the technique used for the electro-acoustic loudspeaker to maximize efficiency. The back volume (V_b) filled with the working gas, which act as a gas spring. It is an arrangement made for the loudspeaker to match its operating frequency (f_d) with the resonator frequency f. The loudspeaker with the back volume gas spring system is known as the driver. The back volume of the gas spring system is given by:

$$V_b = \frac{\gamma P A_b^2}{s} \tag{21}$$

where γ is the specific heats ratio, P is the average gas pressure (same as working gas in the resonator), A_b is the cross-section of the back volume system. The back volume (V_b) is proportional to square of the cross-section of the back volume system and inversely proportional to the gas spring stiffness s. It is found in the recent research that the driver with piston diameter d_p (vibrating diaphragm) is desirably equal to the diameter of the large diameter resonator tube [2]. By providing back volume system, the stiffness of the gas spring is matched with the mechanical stiffness of the driver [19]. This matches the driver frequency (f_d) with resonator frequency (f). The same piston

Table 7. Electromechanical parameters of the acoustic driver attached to the 50 W TSDH and TDH resonators design.

A_p = 75.43 cm^2, R_e = 4 Ω, L_e= 0.0013 H, Bl = 25 T-m, m = 25 g, s = 157.9 kN m^{-1}, R_m = 3 Ns m^{-1}

Table 8. Thermo-physical properties of the refrigerator components materials (at P = 10 bar, T_{mg} = 266 K and f = 400 Hz) chosen in the DeltaEC simulation modelling.

Component type	Preferred solid material	Density (kg m^{-3})	C (J kg^{-1} K^{-1})	k (Wm^{-1} K^{-1})	δ (m)
Stack	Kapton	1422.4	968.2	0.186	1.0367e−05
	Mylar	1353.5	984.2	0.155	9.6296e−06
Heat exchangers (CHX/HHX)	Copper	9000	420	399.9	2.9016e−04
Resonators/driver	Ideal/Celcor	2510	686.8	2.5	3.3972e−05
	Stainless	7930.3	437.6	13.7	5.6070e−05

Table 9. DeltaEC simulation performance results at 3% drive-ratio of the λ/3-TSDH and λ/4-TDH resonator designs showing the importance of stack in the resonator system.

Resonator design	T_{mg} (K)	f (Hz)	W_e (W)	η_{ea} (%)	Q_r (W)	T_{cx} (°C)	θ_x (K)	COP	COPR
λ/3-TSDH (with stack)	286	463	83.1	81	133.1	− 3.4	31.4	0.882	0.294
λ/3-TSDH (without stack)	303	483	42.7	52.4	92.7	30	− 2.0	2.744	0.915
λ/4-TDH (with stack)	286	480	83.5	81.2	133.5	− 4.3	32.3	0.841	0.280
λ/4-TDH (without stack)	303	493	42.4	52.2	92.4	29.9	− 1.9	2.667	0.889

diameter may be used in the back volume gas spring system ($d_b = d_p$) (figure 1). The electromechanical parameters of the driver are given in table 7 and by substituting the known values in Eq. (21) at 10 bar pressure, the back volume V_b is found to be 602 cc. The design and optimization procedure for the commercially available loudspeaker can be found elsewhere [4, 6].

5. DeltaEC modelling results and analysis

The DeltaEC stands for design environment for low-amplitude thermoacoustic energy conversion is a modelling and simulation software specially designed for thermoacoustic engines and refrigerators [15, 20]. The DeltaEC uses computer programme that integrates the one-dimensional wave equation, heat flow equation and acoustic power flow equation in a gas or a liquid for the complex geometry developed by the designer. It is used to simulate the performance behaviour of the theoretically designed thermoacoustic devices (engines or refrigerators). The DeltaEC models can make use of the following sequence of thermoacoustic segments: loudspeaker, ducts, HHX, CHX, stack, cones, compliances, etc. All the thermoacoustic segments are assumed to have insulation wrapped around their side-wall boundaries by default and hence the HHX has to reject the heat energy (Q_r) input to the CHX as the heating load (Q) and the electrical energy input to the loudspeaker (W_e). The electrical energy input to loudspeaker is the sum of acoustic energy input to the resonator (W) and the heat energy loss during energy conversion. For every thermoacoustic segment, the integration is done using the segment local parameters such as the length, area, and perimeter and global parameters such as the average gas pressure, operating frequency of the refrigerator, initial temperature of the working gas, and the volume velocity of the oscillating gas. It assumes isothermal except in the stack and stack duct segments. The user can set the guesses and targets for the required segment parameters. It also uses Reverse Polish Notation (RPN), a parenthesis-free algebra encoding technique. The user can define RPN segments at the end of the programme part to determine the required output parameters. The user has to iteratively adjust the guesses variables in the programme to satisfy the required targets. The detailed explanation regarding the design of thermoacoustic refrigerator using the DeltaEC software with text files can be found elsewhere [8, 15]. By using the data given in tables 2 and 7 and the resonator designs shown in figures 4 and 5 are validated using DeltaEC software. The thermo-physical properties of the best component materials used in building the DeltaEC simulation models are given in table 8. The DeltaEC simulation performance results for the 50 W λ/3-TSDH and λ/4-TDH resonator designs at 3% drive-ratio showing the importance of stack in the resonator system are given in table 9. The no stack refrigerators show better COP at higher CHX temperature (T_{cx}) because of the fluid turbulence in the resonator system compared to the stack-based systems. Therefore, the stack-based refrigerator systems are preferred for obtaining better CHX temperature at lower COP (Table 9). The simulation results as a function of the cooling power and drive-ratio for an alternate and efficient λ/4-TDH resonator design are given in table 10. From the simulation results we can interpret that at lower cooling power, the refrigerator shows lower COP and lower CHX temperature, and vice-versa. The results also show that the higher drive-ratio (6%) is better for achieving lowest CHX temperature at lower COP compared to 3% drive-ratio but operating the refrigerator with 6% drive-ratio depends on the force factor (Bl) of the loudspeaker as discussed

Table 10. DeltaEC simulation performance results of the $\lambda/4$-TDH resonator design (with stack) as a function of cooling power and drive ratio.

Q (W)	D (%)	T_{mg} (K)	f (Hz)	W_e (W)	η_{ea} (%)	Q_r (W)	T_{cx} (°C)	θ_x (K)	COP	COPR
10	3	255	426	59.7	69.5	69.7	− 65.6	93.6	0.367	0.122
	6	250	414	420.3	34	430.3	− 78.6	106.6	0.206	0.069
20	3	263	442	65.6	73.6	85.6	− 49.1	77.1	0.532	0.177
	6	252	418	427.5	35.2	447.5	− 74.1	102.1	0.266	0.089
30	3	271	456	71.5	76.8	101.5	− 33.5	61.5	0.658	0.219
	6	254	423	434.6	36.2	464.6	− 69.6	97.6	0.321	0.154
40	3	279	468	77.5	79.3	117.5	− 18.6	46.6	0.758	0.253
	6	257	427	441.8	37.2	481.8	− 65.2	93.2	0.371	0.124
50	3	286	480	83.5	81.2	133.5	− 4.3	32.3	0.841	0.280
	6	259	431	448.9	38.2	498.9	− 60.8	88.8	0.417	0.139

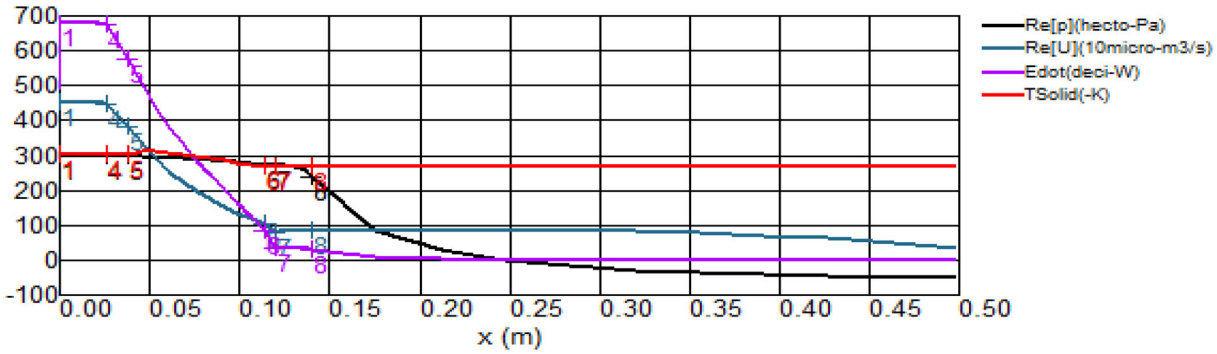

Figure 6. A DeltaEC simulation results of a 50 W, λ/4-TDH resonator design showing the variation of: dynamic pressure amplitude P_a (i.e., Re[p]), volume velocity U (i.e., Re[U]), acoustic power input W_a (i.e., Edot), and solid material temperature T_s (i.e., TSolid), along the length of the resonator system.

elsewhere [19, 21, 22]. The variation of dynamic pressure amplitude P_a, volume velocity U, acoustic power input W_a and solid material temperature T_s, along the length of a 50 W, λ/4-TDH resonator design is shown in figure 6.

6. Conclusion

The thermoacoustic refrigerators found in the literature till date are the laboratory scale models with a cooling capacity less than or equal to 10 W [23]. In this research work an attempt is made to design 50 W refrigerators for a temperature difference of 75 K. The design, analysis and optimization of the spiral stack-heat exchangers' system, and λ/3-TSDH and λ/4-TDH resonator designs and the back volume gas spring system for the loudspeaker are discussed. The stack-heat exchangers' system is optimized based on the minimum acoustic power consumption (43.7 W, table 4). The minimum acoustic power loss W_2 (4.526 W) for the λ/3-TSDH resonator design in the small diameter tube is found at a diameter-ratio (d_2/d_1) of 0.8. At this condition the VRT of 6.73 L is provided to simulate an open end where VRT = 7.44 VLT. The diameter-ratio of 0.2 is provided for an alternate and compact λ/4-TDH resonator design with a VRT of 6.27 L (6.93 times VLT) which is sufficient to simulate an open end in the buffer volume [2, 3, 7].

The λ/4-TDH design shows 16% decrease in resonator surface area (A_t), and 6.7% decrease in volume (V_t), leading to 7.2% improvement in the power density P_v and 2.9% increase in COP compared to the λ/3-TSDH design.

The optimized λ/3-TSDH and λ/4-TDH resonator designs are validated using the DeltaEC software. The DeltaEC modelling results for both the resonator designs show that the temperature of the CHX and COP increases drastically in the absence of stack (table 9) because of fluid turbulence in the resonator system. The temperature of the CHX (T_{cx}) and COP increases with increase in cooling load and vice versa (table 10). The DeltaEC predicts that the refrigerator performance at 6% drive-ratio is better compared to 3% drive-ratio. But the drive-ratio depends on the force factor (Bl) of the loudspeaker to generate the required

acoustic pressure amplitude P_a in the resonator system as discussed elsewhere [2, 6].

The theoretically optimized and DeltaEC validated λ/3-TSDH and λ/4-TDH resonator designs may be fabricated to validate the real performance of the acoustically-driven 50 W thermoacoustic refrigerators similar to 10 W thermoacoustic refrigerators found in the published literature [1] as the future scope.

Acknowledgements

This work was supported by JSSMVP Mysuru, Principal, HOD (IEM) and all staff of the Department of Industrial Engineering and Management, JSSATE Bengaluru. Authors thank Bill Ward, John Clark, and Greg Swift, Los Alamos National Laboratory, USA for developing DeltaEC software and making it freely available for research purpose.

List of symbols

A	Cross-sectional area of the stack, m^2
A_p	Cross-sectional area of the loudspeaker piston, m^2
A_t	Total resonator surface area, cm^2
Bl	Force factor, NA^{-1} or T-m
CDH	Convergent and divergent section with hemispherical end
CHX	Cold heat exchanger
COP	Coefficient of performance
COPC	Carnot's coefficient of performance
COPR	Coefficient of performance relative to Carnot's
C_{ph}	Isobaric specific heat of helium gas, J kg^{-1} K^{-1}
D	Drive-ratio
d_1	Large diameter tube, mm
d_2	Small diameter tube or throat diameter, mm
f	Resonator frequency, Hz
f_d	Driver frequency, Hz
HHX	Hot heat exchanger
k_h	Thermal conductivity of helium gas, Wm^{-1} K^{-1}
k	Wave number, rad m^{-1}
L_e	Driver electrical inductance, H
L_t	Total resonator length, mm
l	Half spiral stack sheet thickness, mm
l_1	Distance between loudspeaker and hot end of the stack, mm
l_2	Distance between loudspeaker and hot heat exchanger, mm
l_3	Length of hot heat exchanger, mm
l_4	Length of stack, mm
l_5	Length of cold heat exchanger, mm
m	Driver moving mass, kg
P	Average gas pressure, bar
P_a	Acoustic or dynamic pressure amplitude, bar
P_v	Power density, Wm^{-3}
p_1	Acoustic pressure amplitude at a particular location, Nm^{-2}
Q	Cooling power or cooling load at cold heat exchanger, W
Q_r	Heat rejected by hot heat exchanger, W
R_e	Driver electrical resistance, Ω
R_m	Driver mechanical resistance, Nsm^{-1}
s	Spring stiffness, kN m^{-1}
TDH	Taper and divergent section with hemispherical end
TSD	Taper and small diameter tube with divergent end
TSDH	Taper, small diameter tube and divergent section with hemispherical end
T_{cx}	Temperature of the cold heat exchanger, K
T_{hx}	Temperature of the hot heat exchanger, K
T_{mg}	Mean temperature of gas across heat exchangers, K
u	Velocity of sound, ms^{-1}
u_1	Velocity amplitude at a particular location, ms^{-1}
V_b	Back volume of the loudspeaker, cc
W_a	Acoustic power input to resonator system, W
W_e	Electrical power input to loudspeaker, W
W_{cx}	Acoustic power dissipated in the cold heat exchanger, W
W_{hx}	Acoustic power dissipated in the hot heat exchanger, W
W_{sx}	Acoustic power dissipated in the stack-heat exchangers system, W
W_2	Total acoustic power loss in the small diameter tube, W
X	Stack center position, mm
x	Position along sound propagation in the resonator tube, mm
y	Half spiral stack sheet spacing, mm
η_{ea}	Electroacoustic efficiency of the loudspeaker, %
λ	Wavelength, mm
μ_h	Dynamic viscosity of helium gas, kg m^{-1} s^{-1}
θ_x	Temperature difference across the hot and cold heat exchangers, K
θ_c	Critical temperature difference across the stack length, K
θ_2	Diverging angle in the buffer volume, degree
δ_k	Thermal penetration depth, mm
δ_v	Viscous penetration depth, mm
ε	Porosity of the stack
γ	Ratio of specific heats
β	Thermal volumetric expansion coefficient, K^{-1}
Γ	Normalized temperature difference
Π	Perimeter of the stack-heat exchangers system, mm
Λ	Helium gas conduction correction factor
σ	Prandtl number
ρ_h	Density of helium gas, kg m^{-3}

References

[1] Prashantha B G, Govinde Gowda M S, Seetharamu S and G S V L Narasimham 2017 Design construction and performance of 10 W thermoacoustic refrigerators. *Int. J. Air-Cond. Refrig.* 25(3): 1750023. https://doi.org/10.1142/s2010132517500237

[2] Prashantha B G, Govinde Gowda M S, Seetharamu S and G S V L Narasimham 2017 Design and comparative analysis of thermoacoustic refrigerators. *Int. J. Air-Cond. Refrig.* 25(1): 1750002. https://doi.org/10.1142/s201013251750002x

[3] Swift G W 1988 Thermoacoustic engines. *J. Acoust. Soc. Am.* 84(4): 1145–1180

[4] Tijani M E H 2001 *Loudspeaker-Driven Thermo-Acoustic Refrigeration*. Ph.D. Thesis, Eindhoven University of Technology.

[5] Prashantha B G, Govinde Gowda M S, Seetharamu S and G S V L Narasimham 2013 Theoretical evaluation of 10-W cooling power thermoacoustic refrigerator. *Heat Transf. Asian Res. J.* https://doi.org/10.1002/htj.21094

[6] Prashantha B G, Govinde Gowda M S, Seetharamu S and G S V L Narasimham 2013 Theoretical evaluation of loudspeaker for a 10-W cooling power thermoacoustic refrigerator. *Int. J. Air-Cond. Refrig.* 21(4): 1350027. https://doi.org/10.1142/s2010132513500272

[7] Prashantha B G, Govinde Gowda M S, Seetharamu S and G S V L Narasimham 2013 Design and analysis of thermoacoustic refrigerator. Int. J. Air-Cond. Refrig. 21(1): 1350001. https://doi.org/10.1142/s2010132513500016

[8] Prashantha B G, Govinde Gowda M S, Seetharamu S and G S V L Narasimham 2013 Effect of mean operating pressure on the performance of stack-based thermoacoustic refrigerator. *Int. J. Therm. Environ. Eng.* 5(1): 83–89, https://doi.org/10.5383/ijtee.05.01.009

[9] Tijani M E H, Zeegers J C H and de Waele A T A M 2002 Design of thermoacoustic refrigerators. *Cryogenics* 42: 49–57

[10] Tijani M E H, Zeegers J C H and de Waele A T A M 2002 The optimal stack spacing for thermoacoustic refrigeration. *J. Acoust. Soc. Am.* 112(1): 128–133

[11] Tijani M E H, Zeegers J C H and de Waele A T A M 2002 Construction and performance of a thermoacoustic refrigerator. *Cryogenics* 42: 59–66

[12] Poese M E and Garrett S L 2000 Performance measurements on a thermoacoustic refrigerator driven at high amplitudes. *J. Acoust. Soc. Am.* 107(5): 2480–2486

[13] Olson J R and Swift G W 1994 Similitude in thermoacoustic. *J. Acoust. Soc. Am.* 95(3): 1405–1412

[14] Prashantha B G, Govinde Gowda M S, Seetharamu S and G S V L Narasimham 2016 Design analysis of thermoacoustic refrigerator using air and helium as working substances. *Int. J. Therm. Environ. Eng.* 13(2): 113–120. https://doi.org/10.5383/ijtee.13.02.006

[15] Swift G W 2002 *Thermoacoustics: a unifying perspective of some engines and refrigerators*. Acoustical Society of America, Melville

[16] Wetzel M and Herman C 1997 Design optimization of thermoacoustic refrigerator. *Int. J. Refrig.* 20(1): 3–21

[17] Hofler T J 1986 *Thermoacoustic Refrigerator Design and PERFORMANCE*. Ph.D. thesis, University of California, San Diego

[18] Garrett S L, Adeff J A and Hofler T J 1993 Thermoacoustic refrigerator for space applications. *J. Thermophys. Heat Transf.* 7: 595–599

[19] Tijani M E H, Zeegers J C H and de Waele A T A M 2002 A gas-spring system for optimizing loudspeakers in thermoacoustic refrigerators. *J. Appl. Phys.* 92(4): 2159–2165

[20] Ward B, Clark J and Swift G W 2008 Design Environment for Low-Amplitude Thermoacoustic Energy Conversion (DeltaEC software). Version 6.2, Los Alamos National Laboratory. http://www.lanl.gov/thermoacoustics

[21] Prashantha B G, Govinde Gowda M S, Seetharamu S and Narasimham G S V L 2015 Resonator optimization and studying the effect of drive ratio on the theoretical performance of a 10-W cooling power thermoacoustic refrigerator. *Int. J. Air-Cond. Refrig.* 23(3): 1550020. https://doi.org/10.1142/s2010132515500200

[22] Prashantha B G, Govinde Gowda M S, Seetharamu S and G S V L Narasimham 2014 Design and optimization of a loudspeaker-driven 10 W cooling power thermoacoustic refrigerator. *Int. J. Air-Cond. Refrig.* 22(3): 1450015. https://doi.org/10.1142/s2010132514500151

[23] Zolpakar N A, Mohd-Ghazali N and EI-Fawal M H 2016 Performance analysis of the standing wave thermoacoustic refrigerator: a review. *Renew. Sustain. Energy Rev.* 54: 626–634